



## **3D Numerical Simulation Analysis for desilting tunnel of Shihmen Reservoir**

**Ming-Lung Li, Ho-Cheng Lien, Shou-I Chen, Yao-Cheng Kuo and Chaur-Gong  
Jong**

### **Abstract**

In the rehabilitation project for the pressure steel pipes of the power plant in Shihmen Reservoir, the pipe is rebuilt to be a desiltation pipe. It is expected that the silt in the reservoir can be moved to the downstream so as to enhance the capacity of the Shihmen reservoir and associated power plant according to the desiltation strategy. Recently, the computation speed of the computer is largely improved so that the 3D numerical simulation can be easily implemented for the full-scale physical experiment in order to investigate the applicability of the 3D numerical model on the hydraulic structure. Therefore, this study aims at adopting a commercial 3D numerical model, i.e. ANSYS CFX, validate the results from the hydraulic model test carried out by Water Resources Planning Institute in 2008 are used as a validation case. In this study, the comparison between the physical model and the numerical model would be made by taking into account the infiltration ratio of trash rack K value. The results of the model validation indicate that the pressure values at different positions calculated by the numerical model are consistent with the results from the physical model. This implies the numerical model can capture the behavior of the pressure estimated by the physical model and provides the detail analysis for the flow field.

Keywords: desilting tunnel, 3D numerical simulation

### **1 Introduction**

Shihmen Reservoir has operated for fifty years since 1963s, it contains five goals that supply for water, irrigation, electricity production, sightseeing, and flood protection. These not only push for local commercial development but protect Taipei from flood, Shihmen Reservoir is the important facility for country.. After the 921 earthquake , it cracked the debris in catchment, and the water in Shihmen Reservoir had been turbid which happened for the other hurricane came from 2001 to 2005. As specially for Typhoon Aere, it caused poor supply for water to Taoyuan city, and decreased the effect for the water catchment capacity.

In the rehabilitation project for the pressure steel pipes of the power plant in Shihmen Reservoir, the pipe is rebuilt to be a desiltation pipe. It is expected that the silt in the reservoir can be moved to the downstream so as to enhance the capacity of the Shihmen reservoir and associated power plant according to the desiltation strategy. Recently, the

computation speed of the computer is largely improved so that the 3D numerical simulation can be easily implemented for the full-scale physical experiment in order to investigate the applicability of the 3D numerical model on the hydraulic structure.

## 2 Numerical methods

We assume that the liquid and the air layer drugs mixed flow in the external auditory canal and middle ear cavity. Consider the effect of gravity. In addition, there is no phase transition occurs. Governing equations used to calculate the mixture velocity and pressure phenomena.

Continuity equation

$$\frac{\partial}{\partial t}(\gamma_\alpha \rho_\alpha) + \nabla \cdot (\gamma_\alpha \rho_\alpha \mathbf{u}_\alpha) = \sum_{\beta=1}^{N_p} (m_{\alpha\beta} - m_{\beta\alpha})$$

Momentum equation

$$\begin{aligned} & \frac{\partial}{\partial t}(\gamma_\alpha \rho_\alpha \mathbf{u}_\alpha) + \nabla \cdot (\gamma_\alpha (\rho_\alpha \mathbf{u}_\alpha \otimes \mathbf{u}_\alpha - \mu_\alpha (\nabla \mathbf{u}_\alpha + (\nabla \mathbf{u}_\alpha)^T))) \\ & = \gamma_\alpha (B - \nabla p_\alpha) + \sum_{\beta=1}^{N_p} c_{\alpha\beta}^{(d)} (u_\beta - u_\alpha) + F_\alpha + \sum_{\beta=1}^{N_p} (m_{\alpha\beta} u_\beta - m_{\beta\alpha} u_\alpha), \end{aligned}$$

In the equation,  $\gamma_\alpha$  is the volume fraction for  $\alpha$ ,  $\rho_\alpha$  is the density for  $\alpha$ ,  $\mathbf{u}_\alpha$  is the speed for  $\alpha$ ,  $\mu_\alpha$  is the viscosity for  $\alpha$ ,  $N_p$  is the total number for the phases,  $c_{\alpha\beta}^{(d)}$  is the resistance between the two phases exchange coefficient,  $m_{\alpha\beta}$  is the rate for mass exchange between the phases, and  $p_\alpha$  is the pressure for  $\alpha$ .

The volume fraction must meet the following conditions:

$$\sum_{\alpha=1}^{N_p} \gamma_\alpha = 1$$

In the equation, assume the phases were the same pressure.

$$p_\alpha = p_1 = p, \quad 2 \leq \alpha \leq N_p$$

ANSYS CFX model for the free surface treatment, also has a volume fraction weighting method and the level set method of the function, it can be different for the reservoir water level elevation simulation analysis. Shimen reservoir silting plant improvement projects main goal, the Department will flow into the reservoir during the typhoon's arrival in muddy water plant density flow inlet, the water plant can be contacted by road will be muddy water discharge pipe pressure reservoir. Therefore, the power plant on the 1st penstock connected manifold articulation original two generator sets operate at high water flow 110CMS (per unit for the 55CMS), power plants will be replaced by the 2nd row of sand penstock Road, the design flow is 300CMS, Total emissions from power plants silting improve the design flow 410CMS.

Build computational grid shown in Figure 2. While both accuracy and numerical simulation of computational efficiency, this study also conducted a grid independence test. In this study, the number of grids were built 600,000, 1,000,000 and 1,500,000 the number of grids, each grid in Table 1 is the number of outlet flow simulation, we can see from the table, one million simulations of the number of grids traffic has been with 1.5 million the number of simulation results are consistent grid, display grid number reached 100 million or more as long as it does not affect the accuracy of the simulation results, therefore, this study adopts 1,000,000 number of grids and grid's configuration.

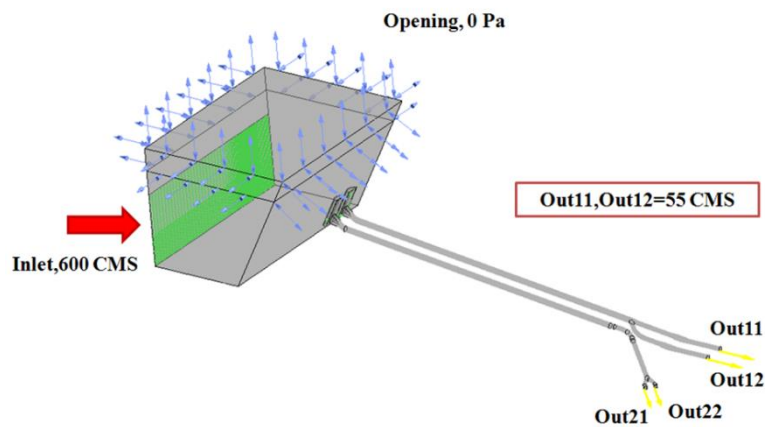


Fig. 1 The 3D numerical simulation boundary condition of reservoir

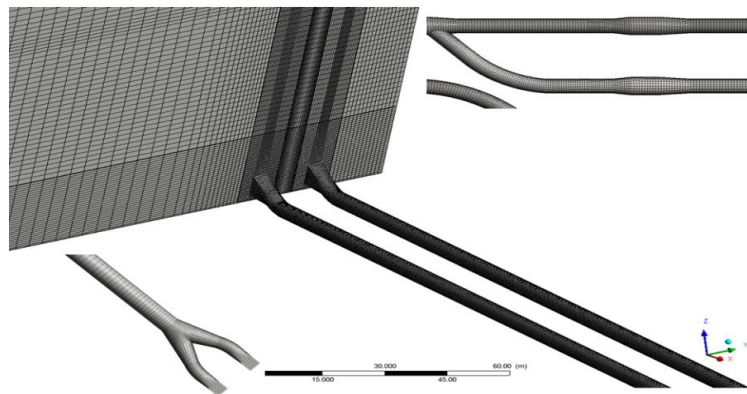


Fig. 2 The computational grid of the 3D numerical simulation

### 3 Flow field analysis

The three-dimensional numerical simulation of the reservoir is carried out for the three-dimensional flow field in the flow field phenomenon of the No. 2 pressure steel pipe drainage channel, the negative pressure zone of the branch pipe, the force of the pipe and the branch pipe flow on the pipe wall, the shear stress of the pipe wall and the mud sand analysis. Analyze and review the distribution of flow fields under different water level elevations, mud sand concentrations and water outlet conditions.

After the rate is determined, the column sand barrier permeability coefficient  $K$  is  $8 \times 10^{-9}$  and the pipe wall roughness  $R$  value is 0.003. We calculate the flow in the No. 2 pressure steel pipe under different outlets and different water level elevations. Field phenomenon.

Observe the velocity vector diagram of the branch pipe of the No. 2 pressure steel pipe in the power plant to the water outlet, as shown in Figure 3. When the fluid flows through the branch pipe, the space velocity suddenly decreases, the fluid velocity decreases, the fluid maintains the inertial flow direction, hits the pipe wall of the pressure steel pipe, and the broken area of the steel pipe becomes smaller, causing the fluid to accelerate inside the branch pipe. A fluid stagnation zone is formed on both sides of the diverging tube, and the fluid velocity here is almost zero. The higher the sediment concentration in the sputum, the higher the fluid density. In theory, the higher the fluid density, the slower the fluid flow rate. However, the weight percentage of the sediment concentration we refer to is very small, and the fluid velocity is not changed. Cause too much change. The numerical simulation results show that the larger the mud sand concentration is, the smaller the fluid velocity is due to the setting of the water outlet boundary. The same water level elevation is small, the outlet pressure is larger, and the pressure difference between the water inlet and the water outlet is smaller. The fluid velocity is also relatively small. The smaller the outlet pressure, the larger the pressure difference between the water inlet and the water outlet, and the higher the fluid velocity

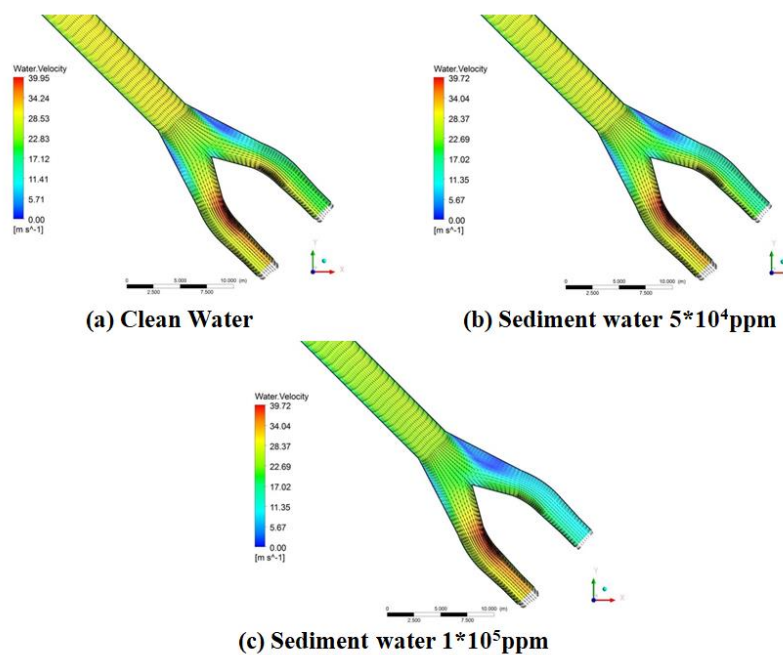


Fig. 3 Local velocity vector distribution near the water outlet

#### 4 Concentration analysis of Sediment

The research team has held a working meeting with the water testers of the Water Regulation Institute for many times, and actually visited the hydraulic test operation

process to understand that during the test, the mudstone concentration attenuation rate of the muddy water is extremely small (less than 5%). The sedimentation effect of muddy sand is not significant. Therefore, in the treatment of three-dimensional numerical simulation, it should be treated with air-hydrophobic two-phase flow, and the hydrophobic part is simulated by the mixed density of water sand.

In this study, the test results of the sand-bearing water concentration of  $5.5 \times 10^4$  ppm (=  $55 \text{ kg/m}^3$ ) provided by the hydraulic test laboratory will be used as a simulation verification case. We first convert the hydrophobic concentration into a volume percentage, and use the volume fraction to calculate the uniform mixing density of the hydrophobic water. The mixing density can be calculated by the following formula :

$$\rho_{\text{mix}} = \frac{(\rho_{\text{water}} \cdot V_{\text{water}}) + (\rho_{\text{sand}} \cdot V_{\text{sand}})}{V_{\text{mix}}}$$

It is calculated that the mixing density of the hydrophobic water is  $1034.2 \text{ kg/m}^3$  when the hydrophobic concentration is  $5.5 \times 10^4$  ppm, and the mixing density of the hydrophobic water is  $1062.3 \text{ kg/m}^3$  when the hydrophobic concentration is  $10^5$  ppm.

Fig.4 shows the pressure distribution along the outlet of the No. 2 pressure steel pipe discharge channel of the power plant under the concentration of  $5.5 \times 10^4$  ppm of water. At the entrance, due to the increased density of the reservoir, the inlet pressure (measured at the first point) will be raised to a height of 58 m (water) at a head height of 54 m (clear water). The simulation results are also consistent with the trend of the measured values. The simulated pressure head is raised from 58 m (clear water) to 60 meters high (water), and the error is about 2 m.

In addition, the simulated and measured values along the process pressure are also quite consistent. As mentioned above, before the 11th point of the measurement position, the position of the steel pipe is sufficient to provide friction loss and convert to pressure energy due to the decrease in the elevation of the steel pipe. Therefore, the simulated pressure head increases along the path; after the 11th point of the measurement position, the pressure energy needs to be used to overcome the friction loss, so the simulated pressure head will become smaller along the path. Overall, from the above comparison results, under the same conditions of K and R values, the verification results of the pressure distribution along the drainage line of the No. 2 pressure steel pipe of the power plant are also very good

On the other hand, in the above-mentioned drowning case, the three-dimensional numerical simulation calculated that the outlet flow rate of the sand discharge channel was 251.4 CMS, which was reduced by 22.8 CMS compared with 274.2 CMS at the time of clear water, which was reduced by about 8.3%, indicating a high sandy water flow. Will reduce the flow of steel pipe drainage

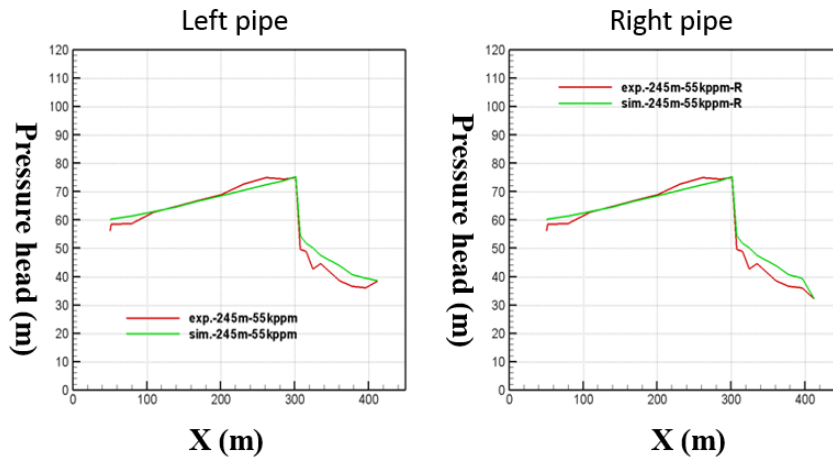


Fig. 4 Distribution of pressure along the outlet of pipe discharge channel of power plant

After completing the verification of the above-mentioned drowning case, we carried out a series of case design and numerical simulations for different power plant outflow conditions, reservoir water level elevation and drowning water concentration conditions. The operation of No. 1 pressure steel pipe of power plant will not affect The outlet flow of the No. 2 pressure steel pipe drainage channel of the power plant is mainly affected by the reservoir water level elevation and the reservoir water concentration (as shown in Figure 5), so the above data is used for regression analysis to obtain the sand drainage channel. The relationship between the drowning flow is as follows :

$$Q = 2 + 1.1zf - 0.000456C$$

Where Q is the flow rate (CMS); zf is the reservoir water level elevation (m); C is the hydrophobic concentration (ppm). The R-square of the above formula is 98.3%, which can provide sufficient precision for subsequent sand volume analysis

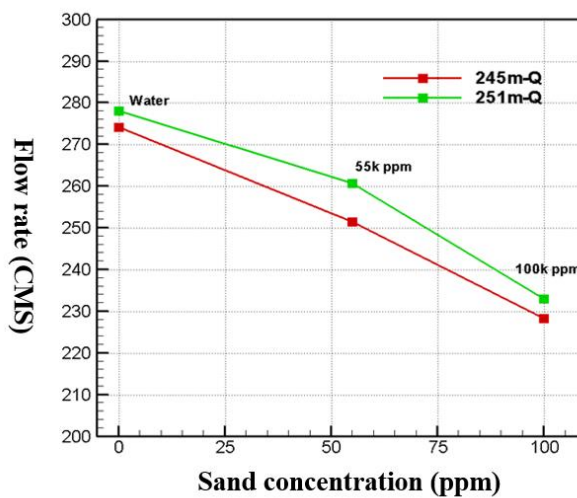


Fig. 5 Relationship between the outlet of the sand discharge channel and the water level elevation and sediment concentration of the reservoir

## 5 Conclusions

In this study, the reservoir water surface elevation, mud sand concentration, and the No. 1 pressure steel pipe of the power plant and the No. 2 pressure steel pipe output of the power plant are defined as the risk factors affecting the pressure distribution of the steel pipe, including the muddy sand concentration, the reservoir water surface elevation and the right end of the power plant No. 2 steel pipe diverging pipe. The outlet flow rate is a sensitive factor affecting the pressure distribution in the steel pipe.

## References

- Alfrink, B.J., and van Rijn, L.C. (1983), "Two-equation turbulence model for flow in trenches," *J. Hydr. Engrg., ASCE*, 109(7), pp.941-958.
- Cokljat, D., and Younis, B.A. (1995), "secondary-order closure study of open-channel flows," *J. Hydr. Engrg., ASCE*, 121(2), pp.94-107.
- Constantinescu, G.S., and Patel, V.C. (1998), "Numerical model for simulation of pump-intake flow and vortices," *J. Hydr. Engrg., ASCE*, 124(2), pp.123-134.
- Demuren, A.O. (1993), "A numerical model for flow in meandering channels with natural bed topography," *Water Resour. Res.*, 29(4), pp.1269-1277.
- Demuren, A.O., and Rodi, W. (1986), "Calculation of flow and pollutant dispersion in meandering channels," *J. Fluid Mech.*, 172(1), pp.63-92.
- Gibson, M.M., and Rodi, W. (1989), "Simulation of free-surface effects on turbulence with a Reynolds Stress model," *J. Hydr. Res., IAHR*, 27, pp.233-244.
- Krishnappan, B.G., and Lau, Y.L. (1986), "Turbulence modeling of flood plain flows," *J. Hydr. Engrg., ASCE*, 112(4), pp.251-266.
- Kuipers, J. and Vreugdenhill, C.B. (1973), "Calculations of two-dimensional horizontal flow," *Rep. SI63, Part I, Delf Hydraulics Lab., Delf, The Netherlands.*
- Leschziner, M.A., and Rodi, W. (1979), "Calculation of strongly curved open channel flow," *J. Hydr. Engrg., ASCE*, 105(10), pp.1297-1314.
- Meselhe, E.A., Sotiropoulos, F., and Patel, V.C. (1995), "Three-dimensional numerical model for open-channels," *Proc., Int. Conf. On Hydropower, Hydropower 95, ASCE*, pp.2100-2120.
- Molls, T., and Chaudhry, M.H. (1995), "Depth-averaged open-channel flow model," *J. Hydr. Engrg., ASCE*, Vol. 121, No. 6, pp. 453-465.
- Neary, V.S., Sotiropoulos, F., and Odgaard, A.J. (1999), "Three-dimensional numerical model of lateral-intake inflows," *J. Hydr. Engrg., ASCE*, 125(2), pp.126-140.
- Noat, D., and Rodi, W. (1982), "Calculation of secondary currents in channel flow," *J. Hydr. Engrg., ASCE*, 108(8), pp.948-968.

**Authors (Text style: Authors Address)**

Ming Lung Li(corresponding Author)

Ho Cheng Lien

Shou I Chen

Yao Cheng Kuo

Chaur Gong Jong

National Center for High-performance Computing (NCHC), Taiwan

Email: long@nchc.narl.org.tw